scientific reports

Check for updates

OPEN

Dimensionless analysis of foam stability for application in enhanced oil recovery

Behnam Dehdari[1], Rafat Parsaei[1]✉, Masoud Riazi[1,2,3] & Mehrdad Niakousari[4]

The stability of foam during injection into oil reservoirs is critical, especially under high-temperature and high-salinity conditions. This study formulates foam stabilizers using one polymer, two surfactants, and six types of nanoparticles (NPs). Foam stability was assessed with a static setup, examining factors such as interfacial tension (IFT), bubble characteristics, and solution viscosity through dimensionless numbers: Bond number (Bo), Worthington number (We), and Neumann number (Ne). A new formula for dimensionless electrical conductivity was also introduced. Results showed that at optimal concentrations of the four additives, foam stability improved with NPs due to enhanced surface charge from in situ physiochemical reactions, promoting their migration to the fluid interface. Notably, Ne proved more effective than Bo and We in describing foam stability as it accounts for droplet height's impact on IFT. Acidic NPs demonstrated greater electrostatic force than amphoteric NPs, correlating with improved foam stability reflected in a downward trend in the Ne plot. Additionally, we analyzed the coarsening rate of foam bubbles over time and its relationship to stability. Our findings suggest that dimensionless numbers serve as valuable benchmarks for evaluating foam stability across various additive mechanisms.

Keywords Bond number, Dimensionless numbers, Foam stability, Modified foam, Neumann number, Worthington number

Because of imbalance between the supply and demand for hydrocarbon fuels on one side and the depletion of oil resources on the other side, applying enhanced oil recovery (EOR) methods are gaining more attention to improve reservoir yields[1–3]. Gas injection is a prevalent process for residual oil recovery after primary and secondary processes[4]; however, it associates with various challenges. For instance, it may not have adequate sweep efficiency due to viscous fingering, and gravity segregation[5]. Various recovery techniques like water-alternative-gas (WAG) are employed to control the mobility of gas in the reservoir. However, WAG suffers from several disadvantages such as the complexities of the operational conditions, high operational costs, and gravity segregation problems[6]. As an alternative method, gas could be injected in the form of foam to control the gas mobility[7,8]. Foam is composed of a continuous liquid phase and dispersed gas phase[9]. Due to the resistance generated by the liquid film (lamella), the foam viscosity is more compared to that of gas, which helps to control high gas mobility[10,11].Thus, foam movement in the porous media is more piston-like especially in heterogeneous porous media, leading to a decent recovery factor. In addition, foams can block the high-permeability paths, and move towards low permeability area[12–16], making foam injection a more suitable candidate for recovering oil from fractured reservoirs. It also increases the capillary number by diminishing IFT and raising the displacing fluid viscosity, which are the main objectives of any EOR method. Other applications of foams include leakage sealing in the gas storage reservoirs[17], aquifer remediation[18], water production control in reservoirs[19], and acid diversion during well stimulation processes[20]. Nonetheless, the thermodynamic instability of foams is a challenging issue, preventing its long-term use in industrial applications[21,22].

Different foam stabilizing agents have been used to enhance the foam stability through different mechanisms including improvement in bubbles durability[23,24] and viscoelasticity[25], reduction in surfactant adsorption in porous media[26], and decrease in foam drainage[27]. In recent years, a mixture of NPs and surfactants have been widely used as foam stabilizer[28,29]. Nanotechnology has provided a new opportunity to apply foam for EOR applications[30–32]. The NPs have prominent characters including the high ratio of surface area to volume, small

[1]Department of Petroleum Engineering, School of Chemical and Petroleum Engineering, Shiraz University, Shiraz, Iran. [2]Enhanced Oil Recovery (EOR) Research Centre, School of Chemical and Petroleum Engineering, Shiraz University, Shiraz, Iran. [3]Present address: Department of Petroleum Engineering, School of Mining and Geosciences, Nazarbayev University, Astana, Kazakhstan. [4]Department of Food Science and Technology, School of Agriculture, Shiraz University, Shiraz, Iran. ✉email: rparsaei@shirazu.ac.ir

size (that prevents blockage of the pore throats), dispensability, and appropriate physicochemical properties[33–36]. Moreover, NPs could decrease gas diffusion between the foam bubbles, preventing bubbles coalescence, and increasing their durability[37–41]. Considering the positive impact of NPs on the foam stability, six acidic and amphoteric NPs (namely SiO_2, Al_2O_3, ZrO_2, TiO_2, Fe_2O_3, and NiO) were used for enhancing foam stability by our research team and the results are available elsewhere[42]. Besides the nanoparticle type, we examined the influence of other factors on foam stability such as pressure, temperature, nanoparticle concentration, polymer and surfactant type and concentration as foam stabilizers.

So far, the stability of foams has been evaluated using various methods such as the data of foam height over time[43–49] and recovery data from core flooding experiments[50–54] and micromodel tests[38–40,55–58]. To better understand the correlation between various parameters and the effect of different phenomena involved in the foam stability, dimensionless numbers were used in this study.

Dimensionless numbers are a set of dimensionless quantities that are employed to analyze the behavior of a system, particularly in fluid dynamics and transport phenomena. Because they allow for the comparison of different systems that may have different physical properties or be operating under different conditions. This approach reduces the number of parameters describing a system, thus subsiding the required number of experimental data for developing empirical correlations[59]. Generally, dimensionless numbers are defined as the proportion of different forces; therefore, they could be employed to clarify the effect of those forces on the process under study[60].

Surface tension force plays the key role on the behaviour of colloidal systems including foam, wherein this force directly affects the formation, shape, and stability of foam bubbles[61]. Furthermore, the gravity forces significantly affect foam shape and stability.

Limited research has explored into the impact of dimensionless numbers on foam stability, particularly within the area of EOR. Recently, Reynolds number (Re) and the Ohnesorge number (Oh) have been used to study foam stability[62,63]. When the flow regime is intermediate ($3\times10^4 < Re < 8\times10^4$), an increase in Reynolds number correlates with foam expansion rates, indicative of enhanced foam stability. Conversely, in turbulent flow regime ($Re > 10^5$), an increase in Reynolds number triggers a decline in foam expansion rate, showing diminished foam stability[62]. Also, high Ohnesorge values corresponded to more stable foams due to increased viscosity and surface tension, preventing the foam bubbles against collapse[63]. The Reynolds number, which is a measure of the ratio of inertial forces to viscous forces, is typically used to predict flow patterns in different fluid flow situations. Although it is important in fluid dynamics, it is less relevant to the specific phenomena of foam stability, which is more influenced by surface tension and gravitational forces rather than inertial forces. Besides, the Ohnesorge number is a dimensionless number that relates the viscous forces to the inertial and surface tension forces. It is often used in the study of droplet dynamics and spray formation. While it is relevant in some aspects of foam formation, it does not directly address the balance of forces that are critical for foam stability, including gravity and surface tension. Consequently, the Bond number, Worthington number, and Neumann number were chosen in this study because of their direct relevance to the forces and dynamics that govern foam stability, making them more suitable than the Reynolds or Ohnesorge numbers for this specific investigation.

Application of dimensional analysis in correlation of data

Bond number

(Bo) is defined as the ratio of gravitational forces to the surface tension force. Worthington first calculated IFT of a droplet under gravity force by measuring drop pressure from a curved droplet in a glass tube[64]. The axisymmetric drop shape analysis (ADSA)[65] was used to measure the surface/interfacial properties of different fluid pairs. This method involves fitting the Young-Laplace equation into the interface of the drop[66,67]. In 1883, Bashforth and Adams[68] presented the numerical solution to the Young-Laplace equation and concluded that gravitational and surface tension forces compete to affect the shape of a pendant drop. Later on, the ratio of gravitational to the surface tension force was named ‘‘Bond Number (Bo)” by Merrington and Richardson in 1947 [69]:

$$Bo = \frac{\Delta\rho g b^2}{\sigma} \tag{1}$$

where σ is the surface/interfacial tension of the fluid pair, Δρ is the density difference between the two fluids, g is the gravitational acceleration, and b is the radius of curvature at the apex of the drop. A high Bond number indicates that the gravitational force is dominant, resulting in more elongated shape of bubbles and drops. Conversely, when the bond number becomes less than one, it shows that the shape of the interface is mainly affected by the surface tension force, resulting in more spherical shapes. Intermediate values of Bond number demonstrate a balance between the surface tension and gravitational forces[70]. Even though not explicitly highlighted in the search findings, we ascertain that the Bond number significantly influences foam stability by characterizing the balance between gravitational and surface tension forces. Understanding and controlling this parameter can lead to improved foam formulations and stability in enhanced oil recovery applications.

Worthington number

(Wo), is a dimensionless number that shows how the bubble volume influences IFT measurement accuracy. It represented the ratio of the actual volume of a bubble (V_d) and maximum bubble volume that should detach from the needle for a given IFT (V_{max}):

$$Wo = V_d/V_max \tag{2}$$

Harkins and Brown described V_{max} as the largest volume of a droplet that can be theoretically preserved by a needle and called it an ″ideal droplet″ expressed as

$$Wo = \frac{\Delta \rho g V_d}{\pi \sigma D_n} \tag{3}$$

where D_n is the needle diameter. Hence, the Worthington number can be expressed as Eq. (4):

$$\mathbf{V_{max}} = \frac{\boldsymbol{\pi}\,\boldsymbol{\sigma}\,\mathbf{D_n}}{\Delta\,\boldsymbol{\rho}\,\mathbf{g}} \tag{4}$$

Wo in Fig. 1 is also considered as Bo with a length scale of $\sqrt{\frac{V_d}{\pi D_n}}$. Berry and co-workers[71] argued that Wo could be used more effectively as a post-measurement "sanity check" to give an important indication of measurement accuracy. This observation highlights the significance of the relative size of droplets and the Wo scale ranging from 0 to 1 when considering the volume effect. Higher values of Wo indicate higher level of precision. Consequently, this can serve as a validation step after measurements to verify the adequacy of the obtained data in terms of accuracy. The higher the precision of the interfacial tension data, the more reliable the stability measurements of the foam. While search outcomes lack comprehensive insights into the Worthington number's impact on foam stability, we show its significance in interfacial tension measurement and droplet formation–a pivotal factor for evaluating and predicting foam stability.

Neumann number

(Ne) demonstrates the impact of the bubble height on IFT. According to Yang et al.,[65] when the droplet volume is very small, the precision of the drop shape analysis and the measurement of IFT by dimensionless number Bo are adversely affected. To address this issue, they proposed Ne as another dimensionless number to consider the impact of the drop height on IFT.

$$Ne = \frac{\Delta\rho\ g\ b\ H}{\sigma} \tag{5}$$

where b is the apex radius of curvature, and H is the drop height.

A low Ne indicates that capillary force is more dominant than the gravitational force. Yang et al., also showed that Bo and Wo produce error in measuring IFT in very small droplets. Consequently, the Neumann number assumes significance in describing foam behavior dynamics, particularly concerning coarsening phenomena within foams. Increased liquid content can block gas diffusion at the Plateau borders, altering the coarsening dynamics and thus the stability of the foam. These three dimensionless numbers are utilized to investigate the accuracy of drop-shaped analysis. The precision of drop-shaped analyses directly influences IFT values and subsequently determines foam stability accuracy. In this context, Wo precision surpasses that of Bo while Ne exceeds Wo accuracy level–thus affirming data validity regarding stability assessments further.

In this study, we employed different dimensionless numbers for describing the foam behaviour in the presence of different chemicals including NPs, surfactants, and polymer using foam half-life time, bubble size and foaming solution viscosity and electrical conductivity data.

Materials and methods

Materials

We used six different NPs (SiO_2, Al_2O_3, ZrO_2, TiO_2, Fe_2O_3, and NiO), one type of polymer [polyvinyl alcohol (PVA)], one type of salt (NaCl), two types of surfactants with different surface charges including cetrimonium bromide (CTAB) and alpha olefin sulphonate (AOS) and a sample of heavy crude oil (μ = 160 cP at 25 ℃). Foaming solutions were prepared using brine at the concentrations of 2, 31, and 60 g/L as well as surfactant,

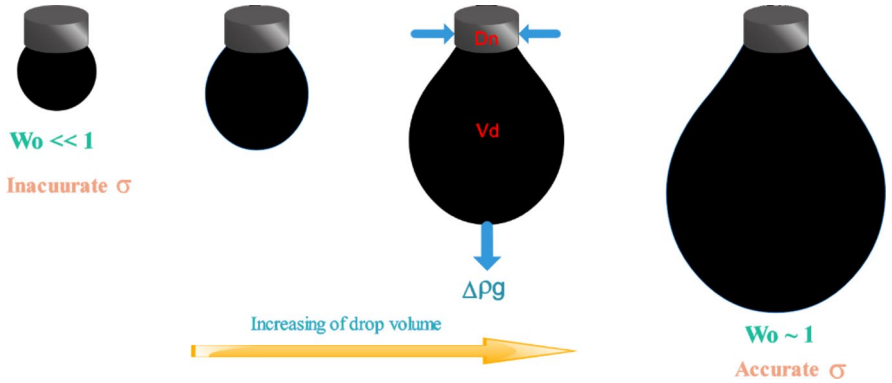

Fig. 1. Effect of drop volume on Worthington number.

polymer, and nanoparticle at three concentrations (0.01, 0.06, and 0.1 wt%). The details of material specifications are available elsewhere[42].

Foam stability, foaming solution viscosity, and bubble size measurement

The experimental procedure for foaming solution preparation, foam generation and stability test is illustrated in Fig. 2. At first, the foaming solution was prepared using different chemicals, then, 100 g/L of the foaming solution was transferred to the glass cell. Next, the nitrogen gas was injected in the cell to create foam, then the injection of gas was stopped and the foam height was recorded over time. All the experiments were performed at operational conditions of 40 °C and 10 bar, and each test was repeated three times to ensure the repeatability of the results. The optimum concentrations of chemicals for achieving maximum foam stability were determined as follows: surfactant (S) = 0.01 wt%, polymer (P) = 0.06 wt%, NPs (N) = 0.06 wt%, and brine (B) = 2 g/L, with more information provided in[42]. The highest foam stability is obtained with Al_2O_3 nanoparticle at a moderate concentration and in the presence of a low concentration of polymer and NaCl. This foaming solution features over 16 times higher half-life time, $t_{1/2}$, compared to the nanoparticle-surfactant system alone.

The changes in surface wettability of various nanoparticles were assessed using the interfacial tension and foam stability data. The results show that Al_2O_3 nanoparticles exhibit a favorable surface area for absorption, compared to the other nanoparticles. This results in partial hydrophobicity of nanoparticles when surfactant adhere to them, subsequently increasing surface elasticity. This ultimately enhances the stability of the lamella and the foam itself. Additionally, the surface tension results reveal that increasing surfactant concentration leads to reduction in equilibrium interfacial tension values due to the Gibbs effect. When the concentrations of surfactant and nanoparticles at the interface of the two fluids are low, their effects on the electrostatic interactions at the solution interface diminishes, resulting in increase in the interfacial tension[42].

A rolling ball viscometer was employed to measure the viscosity of the foaming solution at 40 °C and 10 bar. Also, a high-resolution monochrome camera was utilized to capture snapshots of foam bubbles in order to evaluate bubble size, foam formation time and foam half-life time. The image-J software was applied to determine the distribution of bubble size, the mean bubble size, and the rate of bubble size change. Using the radius of foam bubbles (r) Eq. (6) was applied to calculate the rate of bubble deformation[72]:

$$Rate = \frac{2g\ r^2}{9\ \mu}.\Delta\rho \tag{6}$$

where μ is the viscosity of the foaming solution.

Electrical conductivity measurements

The correlation between electrical conductivity and foam stability is a captivating research area, as electrical conductivity can act as an indirect measure of foam characteristics like liquid content and density. Different properties of surfactant solutions undergo significant changes near their critical micelle concentration (CMC), including IFT as used by Jones et al.[73] for determining the CMC of AOS, and conductivity measurements as applied by Panahpoori et al.[38] for CTAB surfactant. In this study, conductivity data for foaming solution were plotted as a function of surfactant concentration to determine the CMCs. Moreover, electrical conductivity measurements were performed to determine surfactant adsorption on NPs and nanoparticle hydrophobicity.

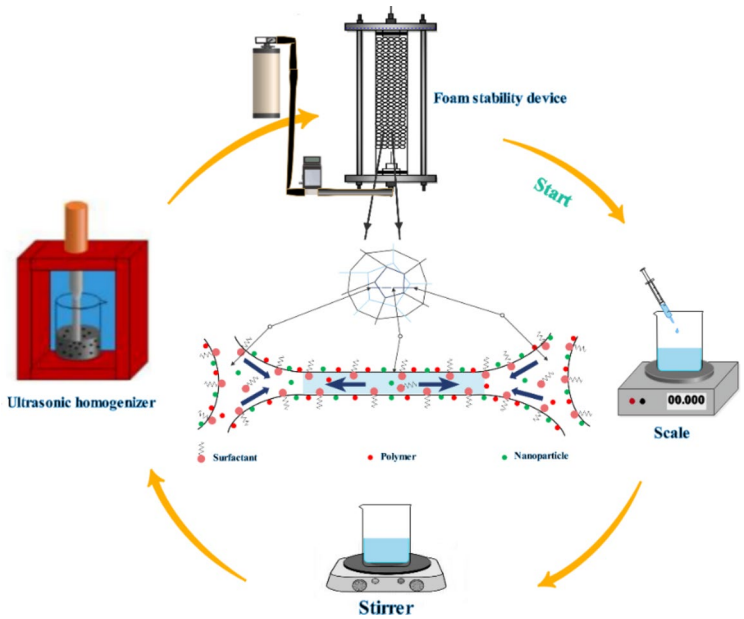

Fig. 2. Schematic of the experimental procedure.

Several solutions were prepared at the optimal concentration of different additives in deionized water, and their conductivity was monitored using a HQ40D53 Portable Multi Meter Conductivity. This device can measure conductivity ranging from 0.01 µS/cm to 20,000 mS/cm with an accuracy of ± 0.5%.

Results and discussion

The stability of the modified foam was evaluated based on the rate of foam bubbles coarsening and electrical conductivity. The behaviour of the modified foam was further elucidated by applying the dimensionless groups such as Bond number, Worthington number, and Neumann number.

The rate of foam bubbles coarsening

The morphology of bubbles was evaluated using the microscopic images of the foam. Foams with different bubble size and high interfacial free energy are thermodynamically unstable. Because charge accumulation on small bubbles is greater than on large bubbles, therefore, mass transfer occurs, leading to a decrease in liquid film thickness and stability. The rate of foam bubble growth over time for different NPs is reported in Fig. 3. As shown, the size of bubbles increases for all cases. Figure 3A and B demonstrate the effect of NPs type on the foam coarsening rate when using polymer in the presence of the anionic and cationic surfactants, respectively. In the presence of ZrO_2, Fe_2O_3, and TiO_2 NPs, a continuous increase of bubble size was observed over time, while in the presence of other NPs, the size changed with lower intensity. Moreover, NiO NPs in the presence of CTAB surfactant show a different trend compared to AOS surfactant. The observed phenomena may be attributed to the strong interaction between NiO, as an acidic nanoparticle, and the cationic surfactant. Consequently, the foam lamellae become closer together and eventually collapse. Generally, in the case of the simultaneous presence of four additives at optimal concentration, the variation in the internal pressure of the bubbles occurs due to the change in their size, which intensifies the Ostwald-ripening phenomenon[74]. Therefore, the bubbles are rapidly connected and the liquid drains out from the foam films due to bubble coalescence. The presence of the amphoteric NPs such as Fe_2O_3 and ZrO_2, not only leads to a lower IFT, but also improves repulsive forces significantly over time, resulting in formation of stable foams. Figure 3A and B also show that Al_2O_3 NPs cause more resistance to bubble size enlargement and hence the highest foam stability because they create higher repulsive forces in the foam lamellae.

The effect of salt concentration on foam bubble growth over time is indicated in Fig. 3C and D, in the absence of nanoparticles. The trend of the two diagrams is ascending for both AOS and CTAB surfactants; nonetheless, this change becomes more significant by increasing the salinity. This is because when polymer and surfactant have similar surface charge, intermolecular forces result in enhancing the viscosity and surface elasticity, therefore, the bubbles do not stick together. These chemicals also increase the electrostatic repulsive force between the charged surfaces. Also, at lower salinity, increasing the Debye length reduces the disjoining pressure, and the bubble deformation occurs at a lower rate. Meanwhile, increasing the salt concentration reduces the flexibility of the polymer molecules, which in turn decreases friction between polymeric chains and increases the intermolecular gravity. This raises the rate of bubble growth. However, excess salts act as a disturbing agent in the system and surfactant molecules move following Le Chatelier's principle[72] to reduce this inconstancy. Therefore, the surfactant molecules do not perform their primary role which is moving to the surface of two fluids. These phenomena ultimately promote the rate of bubble growth and declines the foam stability.

Figure 3E demonstrates how different types of NPs affect the growth rate of the foam bubbles over time in the absence of polymer. According to Fig. 3E, change in the bubble size occurred over time. The lowest change occurred for Al_2O_3 nanoparticle, whereas other NPs caused significant changes in the bubble size. At low anionic surfactant concentration, the hydrophilic NPs do not move to the surface, increasing the attraction dipole-dipole gravity force and adhesion rate of the bubbles. Furthermore, the Debye length and the duration of the fluid remaining in the film reduces due to increasing the adhesion rate of the bubbles; this weakens lamella stability. In the meantime, the utilized NPs were different in size and surface charge. The Al_2O_3 NPs had an appropriate specific surface area (SSA), but this characteristic was not high enough for the other types of NPs. Therefore, the surfactants and ions do not fit properly on the surface, leading to a reduction in surface elasticity[75]. Also, unlike other tested NPs, in the presence of Al_2O_3 NPs, the mass transfer between foam bubbles was low, therefore, the foam bubbles had the least change in size.

Foam stability using dimensionless electrical conductivity

Electrical conductivity was measured for foaming solutions containing salt/surfactants/polymers/NPs, salt/surfactant/polymer, and salt/surfactant/NPs. Using the conductivity data, it is possible to measure the surfactant adsorption on NPs and the hydrophobicity of the nanoparticle. The adsorption index (AI) is calculated as the difference between the total conductivity of soluble components and the conductivity of the solution itself as follows[37]:

$$AI = \{C_{DW} + C_{surfactant\ solution} + C_{brine} + C_{polymersolution} + C_{nanofluid}\} - \{C_{SNP-brine}\} \quad (7)$$

where C is the electrical conductivity. To obtain the dimensionless form of electrical conductivity, we developed the following equation:

$$De = \frac{C}{\rho\,\mu} \quad (8)$$

where ρ is the charge density and can be calculated by dividing the total electric charge (Q) by the volume of the solution (V), having the unit of coulomb per cubic meter (C/m^3). µ is the mobility and shows how easily

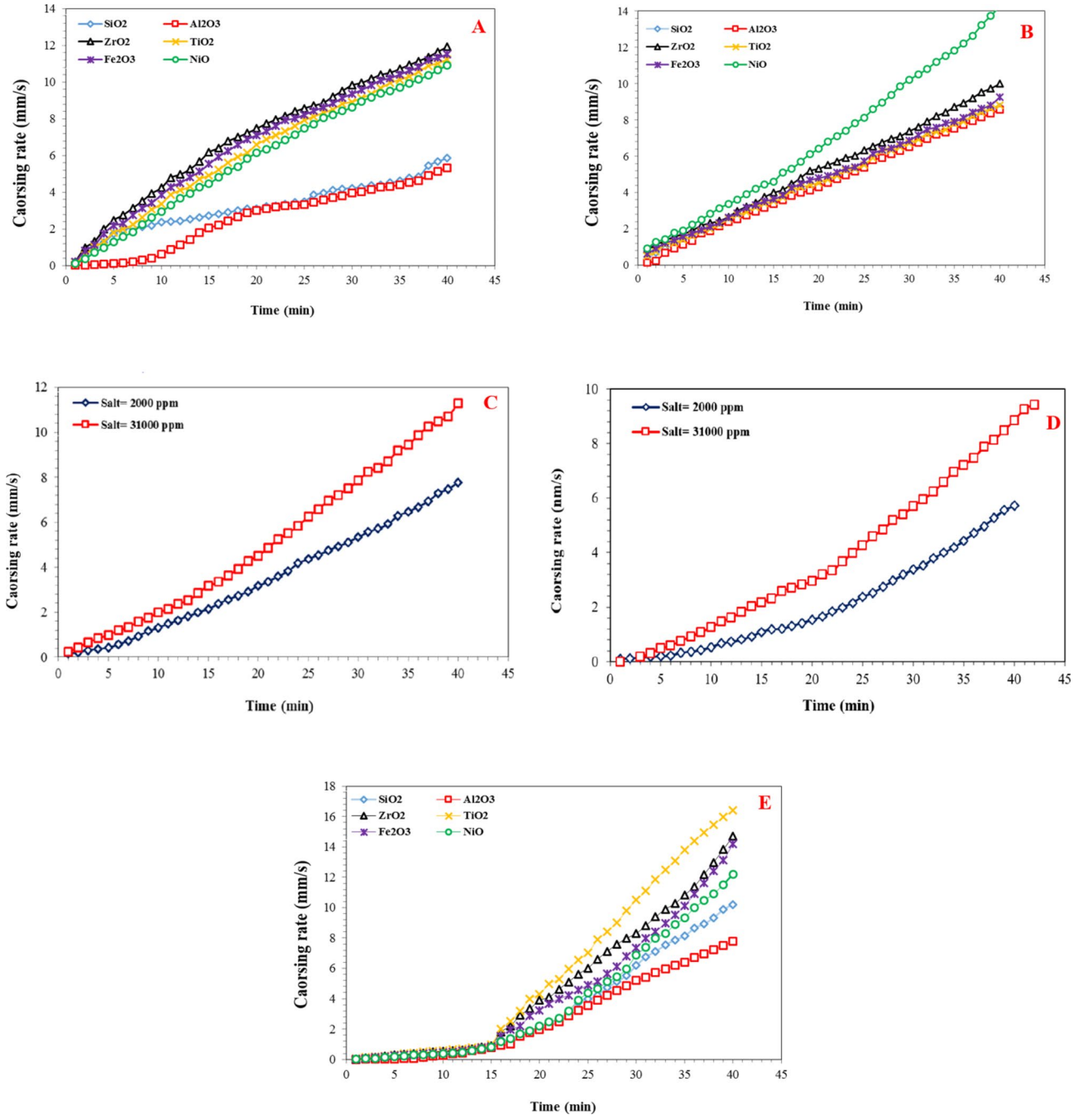

Fig. 3. Rate of foam bubbles coarsening at optimum concentrations of different chemicals: (**A**) SNP, anionic surfactant; (**B**) SNP, cationic surfactant; (**C**) SP, anionic surfactant; (**D**) SP, cationic surfactant; (**E**) SN, anionic surfactant.

charged particles move through a media under the influence of an electric field, with the unit of square meter per volt-second (m^2/V.s). Mobility ($\mu = \frac{V_d}{E}$) represents the charge velocity under an electric field, determined experimentally and calculated from applied voltage. The electrical conductivity of foam closely links to its liquid volume fraction; as liquid content rises, so does the foam conductivity. This connection is crucial since liquid fraction significantly influences foam stability. Higher liquid content generally enhances foam stability by providing a more robust network of liquid films between bubbles.

Figure 4 schematically shows that increasing chemical concentrations after optimal concentration increases the value of conductivity, which is probably because of increasing the number of charged particles. As a result, the adsorption of NPs to the interface decreases, and the foam stability decreases due to increasing the surface gravity forces and reducing osmotic repulsion force[72].

Figure 5A and B indicate the influence of nanoparticle and surfactant type on dimensionless electrical conductivity at the optimal concentration of additives. Among all NPs tested, Al_2O_3 NPs had the greatest change

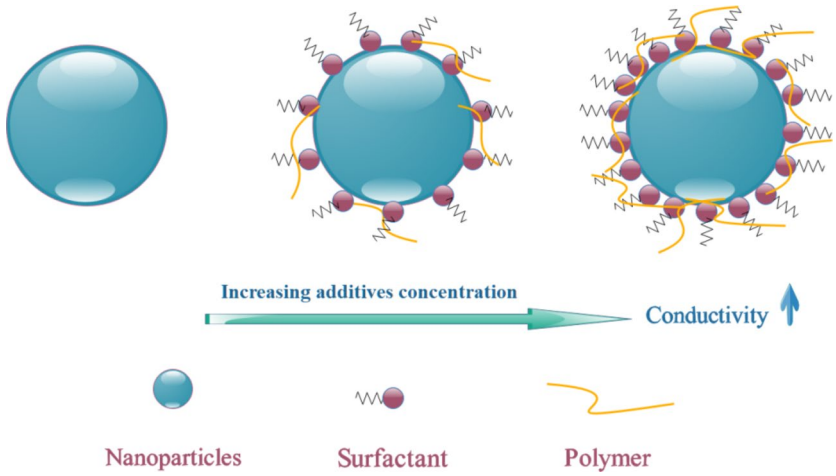

Fig. 4. Schematic representation of nanoparticle hydrophobicity modification by increasing concentration of additives.

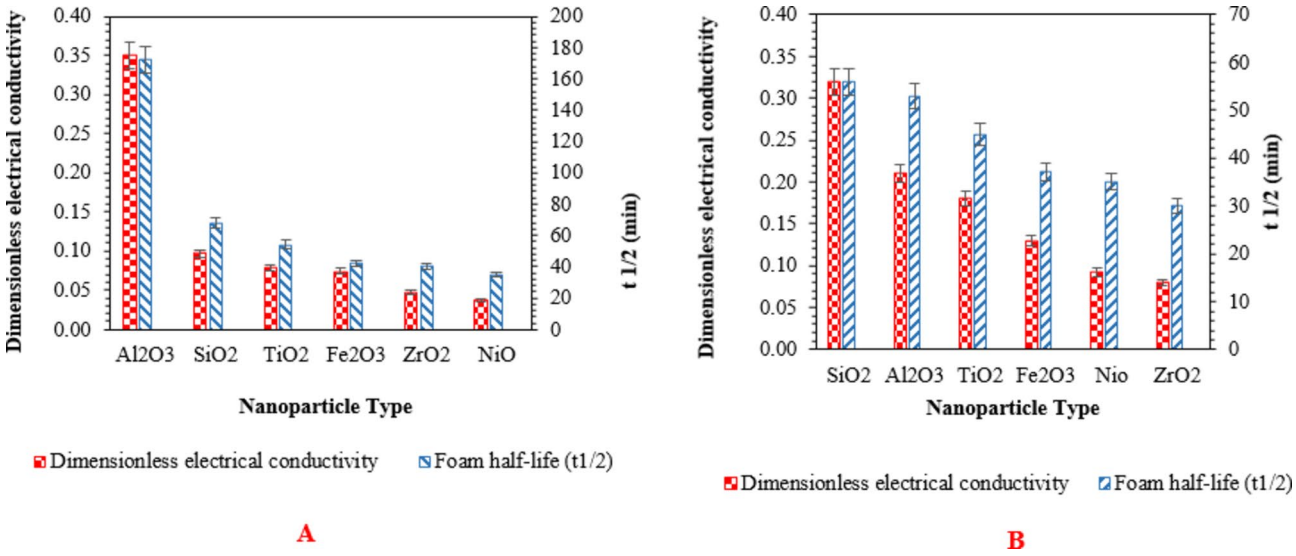

Fig. 5. Effect of nanoparticle type on dimensionless electrical conductivity of SNP-brine at optimum concentration of additives, (A) AOS (B) CTAB.

in surface properties compared to other tested NPs, making them ideal to be coated with surfactant and polymer to achieve maximum hydrophobicity. Therefore, these additives are deposited on the NPs surface, increasing the rate of migration of NPs to the contact surface of two fluids, thereby improving the foam stability. Other NPs are smaller, therefore, fewer surfactant and polymer molecules could adsorb on their surfaces. However, reducing the concentration of these NPs at the fluid pair interface, the charged surfaces become closer[76]. The surface charge of the polymer and CTAB as a cationic surfactant are similar in Fig. 5B. For the Fe_2O_3 NPs, because of changing the surfactant surface charge, the foaming solution has the highest conductivity; however, for the other NPs the surface properties do not have a noticeable alteration. As a consequence, with the addition of surfactant and polymer on Fe_2O_3 nanoparticle surfaces, the conductivity increases, and the NPs become excessively hydrophobic. This causes the NPs to deposit from the interface of the two fluids, and decreases the foam stability. Table 1 demonstrates how salt concentration affects the dimensionless electrical conductivity in the absence of NPs when the surfactant concentration is 0.01 wt% and polymer concentration is 0.06 wt%. According to the results in Table 1, conductivity enhances by increasing the salt concentration due to the effect of monovalent ions and surfactants. However, there exist both the dispersion and ion bonding forces between the molecules of water. Adding electrolyte to the aqueous solution boosts these forces[77]. Although after a certain salinity due to rising the gravitational force, the double layer would be compressed, and instability in the ionic clouds of the charged surfaces happens. In the absence of NPs in foaming solution, the results show that at constant concentrations of surfactants and polymers, conductivity increases by enhancing the brine salinity. Due to the reduction of electrostatic and steric forces, the migration rate of the surfactant molecules to the interface

Salt concentration (ppm)	Surfactant concentration (wt%)	Dimensionless electrical conductivity	Foam half-life time (min)
2000	0.01 (AOS)	0.203 (±0.081)	83.20 (±1.20)
31,000	0.01 (AOS)	6.560 (±1.64)	71.30 (±1.40)
2000	0.01 (CTAB)	0.620 (±0.053)	105.60 (±1.70)
31,000	0.01 (CTAB)	9.850 (±1.15)	93.80 (±1.60)

Table 1 Effect of salt concentration on dimensionless electrical conductivity (polymer concentration: 0.06 wt%).

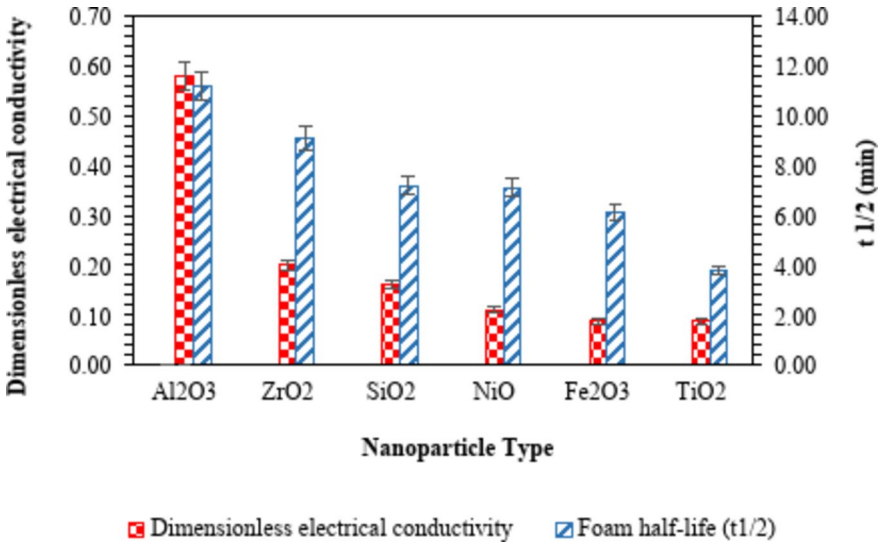

Fig. 6. Effect of nanoparticle type on dimensionless electrical conductivity of SN-brine (anionic surfactant) at optimum concentration.

Salt concentration (ppm)	κ^{-1}(m)
2000	5.22×10^{-9}
31,000	1.32×10^{-9}
60,000	9.49×10^{-10}

Table 2. Values of Debye length at three salt concentrations.

of the two fluids decreases, resulting in a decline in the lamella thickness and the foam stability. The effect of nanoparticle type on the dimensionless electrical conductivity of the foaming solution in the absence of polymer is shown in Fig. 6. Based on the results shown in Fig. 6, TiO_2 NPs result in the highest solution conductivity. In the absence of polymer, the viscosity of foaming solution was smaller and the surfactant movement to the surface of the NPs was easier; therefore, the surface properties of TiO_2 NPs altered properly and they could transfer to the interface of two fluids faster than the other NPs. In the meantime, placing surfactant on the surface of the TiO_2 NPs leads to changing their surface from hydrophobic to hydrophilic, reducing their diffusion rate to the surface and the double-layer forces[78].

Evaluation of foam stability using the bond number

The Bond number is a dimensionless number that shows the balance of the gravity and the capillary forces[79]. In the context of foams, it characterizes the balance between these forces that affect bubble shape and stability. A lower Bo signifies dominance of surface tension forces over gravitational forces, generally promoting foam stability, while a higher Bo indicates gravitational influence, potentially causing drainage and instability. The effect of various types of nanoparticle and surfactant on the Bond number for the foaming solution of (S/P/N/B) at the optimal foam composition is depicted in Fig. 7A and B for the anionic and cationic surfactants, respectively. The Bond number values increase for all NPs in the presence of AOS as an anionic surfactant, indicating that the capillary force overcomes the gravity force and foam stability decreases. Capillary force in an optimum value can improve foam stability[80], beyond which, by increasing capillary force, the electrostatic repulsive force reduces[72]. Moreover, when the gravity force increases, the fluid films become thinner and the

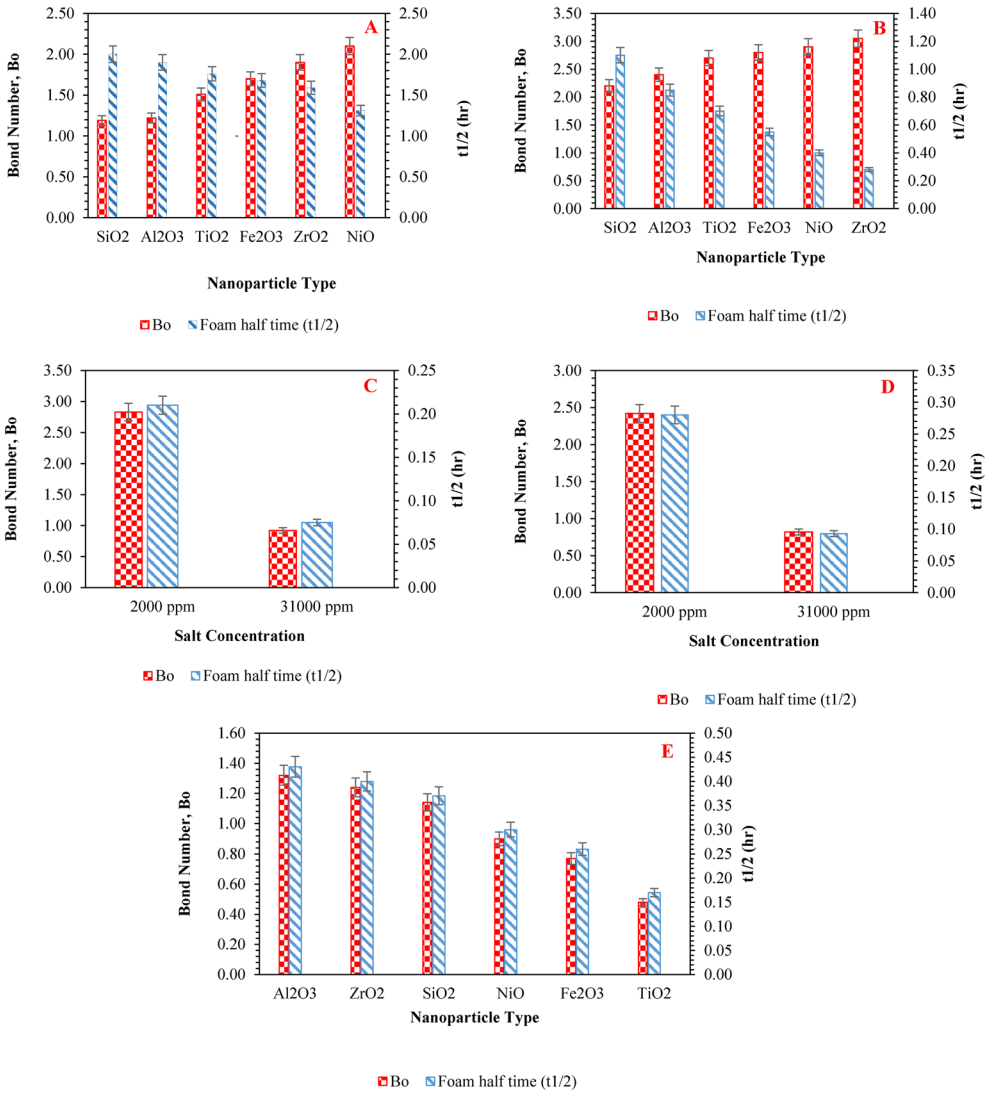

Fig. 7. Bond number versus time: (**A**) SNP, anionic surfactant; (**B**) SNP, cationic surfactant; (**C**) SP, anionic surfactant; (**D**) SP, cationic surfactant; (**E**) SN, anionic surfactant

liquid inside the film stays stable for a shorter period. Besides, the diffusivity of the gas inside the film increases that causes adhesion of the bubbles and ultimately the decay of foam. Figure 7C and D depict the impact of salt concentration and surfactant type on the Bond number at the optimal foam formulation. For this system, no nanoparticle was utilized. Figure 8C shows that the effect of the polymer decreases at a constant concentration of surfactant, in the absence of NPs. Upon rising the salinity, Bo decreases and the drainage rate of liquid from lamella increases.

For understanding the effect of salinity, Debye length (κ^{-1}) can be calculated using Eq. (9) [72]:

$$k^{-1} = \left[5.404 \times 10^{15} \sum_i z_i^2 c_i^{\infty}\right]^{-1/2} \tag{9}$$

where z_i is the valence of the ions dissolved in the solution and c_i^{∞} is the concentration of ions of type i expressed in mol/m^3. The Debye length was calculated at three salt concentrations of 2000, 31,000, and 60,000 ppm and is shown in Table 2. According to Table 2, adding more salt, the value of κ^{-1} decreases. Therefore, increasing the concentration of salt causes the attractive forces to dominate the repulsive forces[72].

When surfactant and polymer have similar surface charge, increasing the salinity leads to increasing the Bond number. The sudden rise of Bo under the salinity of 2000 ppm can be attributed to the London forces that are temporarily dominant, causing the charged surfaces to become separated[81]. On the contrary, increasing salt concentration reduces the viscosity of the solution by placing the Cl^- ion on the polymer surface, which resulted in polymer degradation and polymer chain agglomeration[82]. However, it strengthens the Coulomb

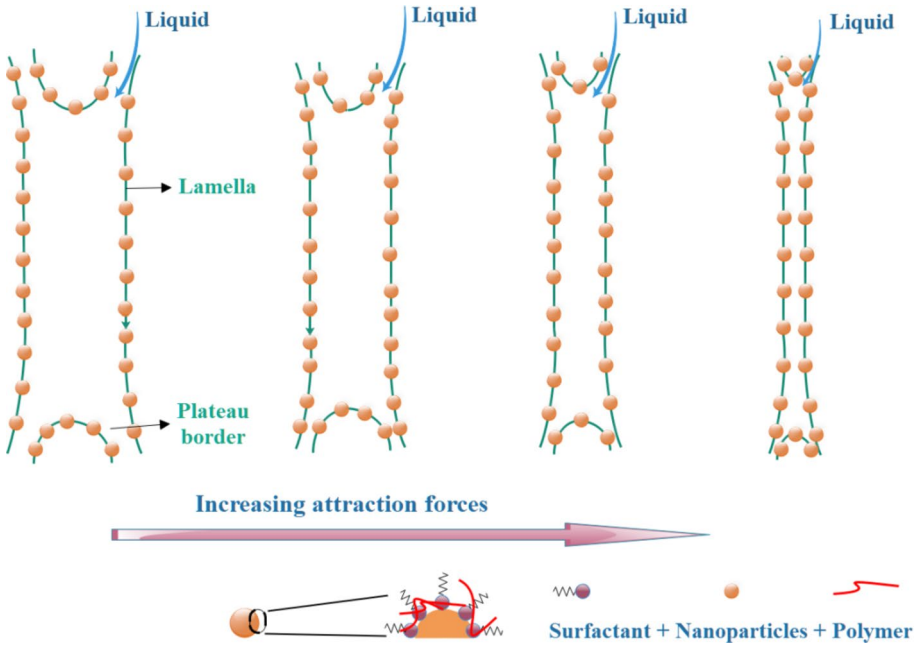

Fig. 8. Schematic of the effect of different chemicals on lamella thickness.

force[72], causing the charged particles to approach each other and push the attractive force to each other. This mechanism is demonstrated schematically in Fig. 8.

Figure 7E indicates the effect of nanoparticle type on the Bond number in the absence of polymer at a constant concentration of anionic surfactant, NPs, and salt. As it is observed, Bo declines over the period shown. Also, all NPs follow a similar trend over the tested period. When the polymer is not present in the system, due to the absence of steric force, the charged surfaces get closer together and the stability decreases. Meanwhile, since the surfactant concentration is low and there is no polymer in the system, the NPs remain in the bulk, therefore, the IFT increases, and subsequently, Bo decreases. A significant decrease in Bo causes a change in the intermolecular forces, and the repulsive force dominates[72]. This decreases the bubbles adhesion rate, which reduces the liquid drainage from the lamella, making the foam more stable.

Evaluation of foam stability using the worthington number

The Worthington number not only reflects the interplay of gravity and surface tension in interface deformation, but also serves as a key dimensionless parameter for evaluating foam stability during droplet and bubble formation processes. In foams, individual bubbles stability (which can be considered as inverted droplets) for overall foam stability. It could be used to determine the position of the charged surfaces by considering the volume of droplet that is extruded from a needle with the diameter of 0.45 mm. Over time, the volume of droplet increased and IFT changed because of the presence of polymer in the aqueous system. The Worthington number is indeed a significant dimensionless parameter that can provide insights into the dynamics of foam generation, particularly in porous media. Wo can reflect the characteristics of foam generation in pores. In other words, the Worthington number depends on the momentum of the fluid, the size of the pores, and the surface tension and viscosity of the gas. These parameters are directly related to the snap-off process, where the size of the pores and the properties of the fluid (such as surface tension and viscosity) play a significant role in determining the stability and size of the bubbles formed. As a result, the Worthington number is a pertinent parameter for understanding foam generation in pores because it captures the essential balance between viscous stress and surface tension, which are fundamental to the snap-off process and the overall dynamics of foam formation. Figure 9A and B indicate the effect of nanoparticle and surfactant types on the Worthington number for the foam of (S/P/N/B) at the optimal foam concentration. As it is presented in Fig. 9A and B, increasing the Wo values resulted in decreasing the foam stability, and the simultaneous presence of four additives creates a retarded condition. The retarded force acts in the direction that the charged surfaces have the maximum distance from each other[72]. Furthermore, NPs form a cork in the plateau border[83], reducing the diffusivity of gas and increasing the bubble stability. Figure 9C and D indicate how salt concentration and surfactant type influence the Worthington number at the optimal foam concentration in the absence of nanoparticles. When the concentration of polymer and surfactant is constant, increasing the salt concentration, the shielding charge phenomenon occurs at the fluid interface[72], which increases the Worthington number. This increase is particularly significant because of the opposite surface charge between surfactant and polymer that decreases repulsive forces. Therefore, Debye length reduction, results in more gas diffusivity and increases the rate of liquid outflow from lamella[84]. Figure 9E demonstrates the impact of nanoparticle type on the Worthington number in the absence of polymer at a constant concentration of salt, anionic surfactant, and NPs. As shown in Fig. 9E, due to the lack of adequate and sufficient stabilizers, the NPs separate from the interface, Wo increases,

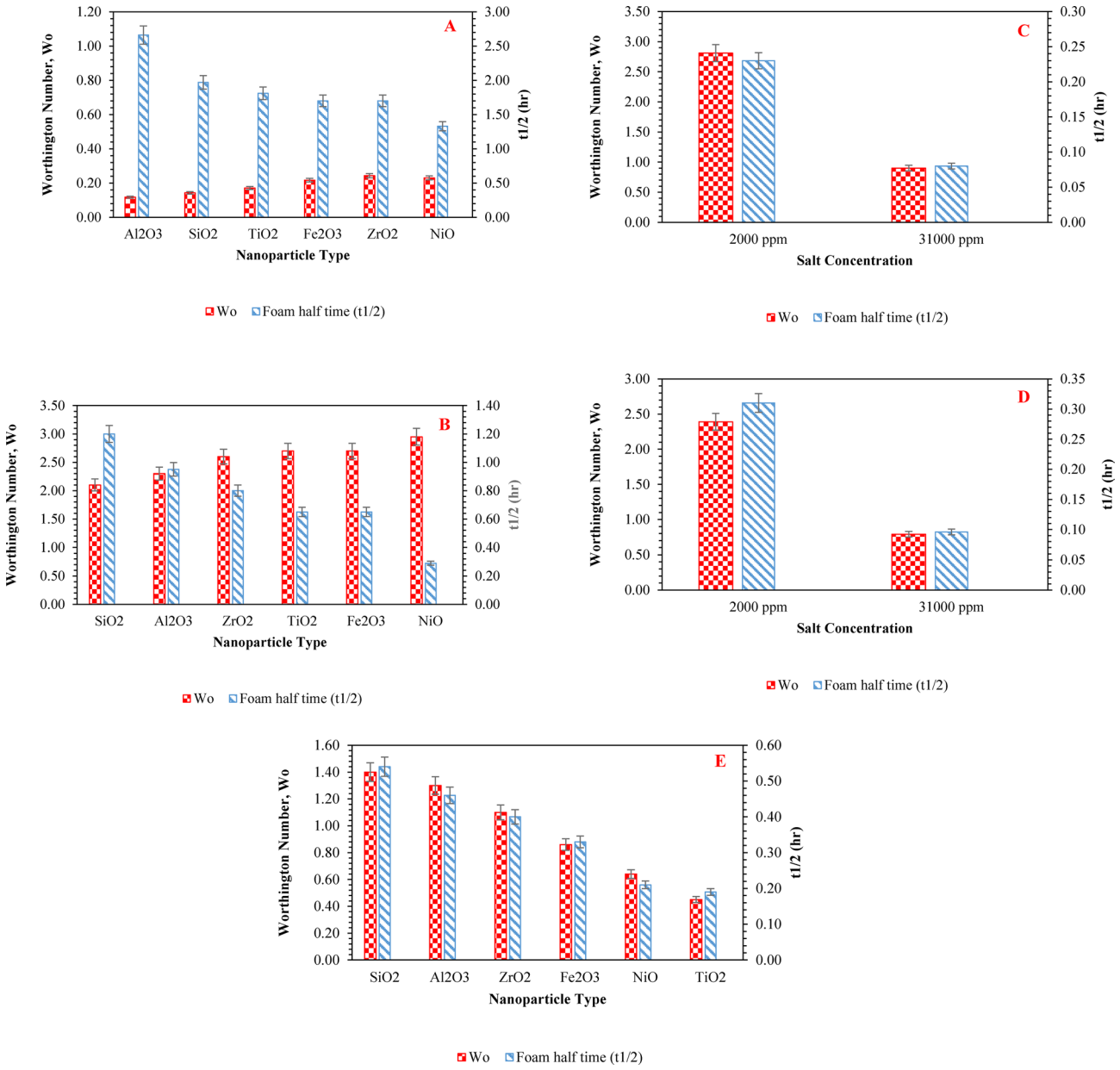

Fig. 9. Worthington number at optimum concentration of additives: (**A**) SNP, anionic surfactant; (**B**) SNP, cationic surfactant; (**C**) SP, anionic surfactant; (**D**) SP, cationic surfactant; (**E**) SN, anionic surfactant.

and foam stability decreases. The Fe_2O_3 NPs, due to their high magnetic properties, deposit on the surface at early times; however, absorbing natural surfactant (asphaltene) of oil leads to Wo increasing relatively. Even though the Fe_2O_3 NPs absorbs asphaltene, mass transfer increases between foam bubbles and alters the bubble size. Consequently, Wo declines and the stability of the lamella increases. The Fe_2O_3 NPs have high adsorption capacity because of their particle size, surface area, and composition; therefore, they can quickly absorb the available asphaltene[85,86]. Due to the fact that the attractive forces overcome the repulsive forces and the foam stability deteriorates, the TiO_2 NPs has the lowest values of Wo. The decrease in Wo does not always mean increased stability and decreased bubble adhesion rates. When Wo decreases or increases greatly, it causes the disjoining pressure gravity force to overcome charged surfaces and to increase the rate of fluid discharge from foam films (i.e., for ZrO_2 NPs).

Evaluation of foam stability using the Neumann number

One dimensionless number that is used to measure foam stability is Ne, which takes into account the height of droplets on the IFT. Besides, the Neumann number is vital in understanding the coarsening process of foams, which involves the growth and shrinkage of bubbles over time. When compared to Wo and Bo, it can represent the position of thin fluid films relative to each other more effectively. Over time, the competition between the gravitational force and the capillary force causes different NPs having a different effect on Ne. Additionally,

it seems that acidic NPs produce more electrostatic force than amphoteric NPs due to the higher pH[42] and lower ionic strength[87]; therefore, charged surfaces are separated and foam stability get improved. The influence of nanoparticle and surfactant type on Neumann number for the solution of (S/P/N/B) at the optimal foam concentration are demonstrated in Fig. 10A and B for the anionic and cationic surfactants, respectively. As can be noticed in Fig. 10A, all NPs except Fe_2O_3 have a downward trend. When Ne decreases, the stability of liquid films decreases and long-range forces dominate in the system. Even though the Fe_2O_3 NPs have lower the IFT, the attractive forces increase among the charged surfaces, and the foam stability decreases. Delaying in the discharge of liquid leads to reducing the bubble coalescence rate and the Ostwald-ripening mechanism, leading to improved durability of the liquid inside the film.

Figure 10C, D depict the effect of salinity and surfactant type on Neumann number when there is no NP in the foaming solution. What is conspicuous from these figures, Ne decreases for both AOS and CTAB surfactants. This reduction of Ne can be related to the surface charge of polymer, which decreases the steric repulsion force

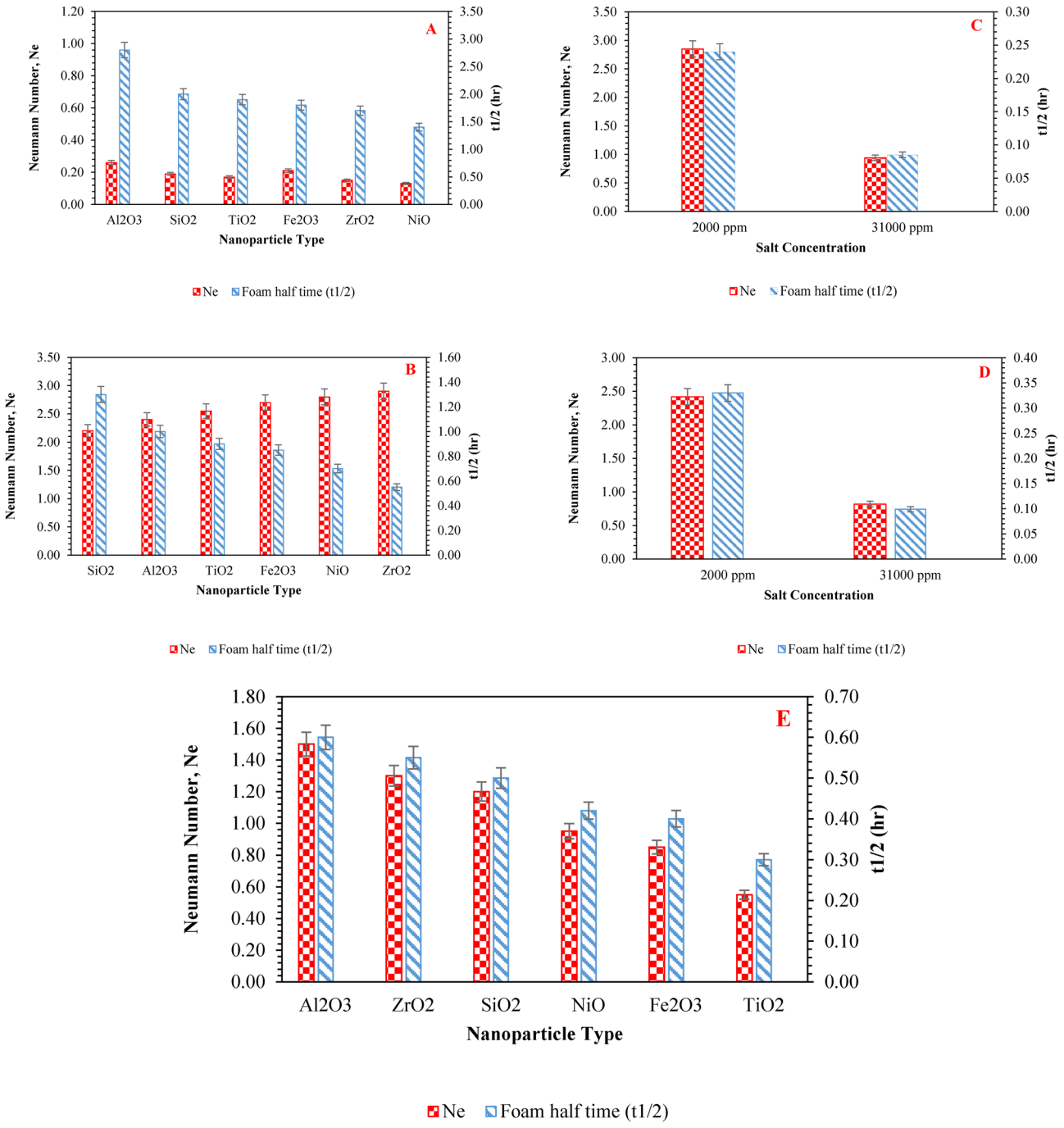

Fig. 10. Neumann number at optimum concentration of additives: (**A**) SNP, anionic surfactant; (**B**) SNP, cationic surfactant; (**C**) SP, anionic surfactant; (**D**) SP, cationic surfactant; (**E**) SN, anionic surfactant.

because of its overlap with the organic chain of surfactant, causing worse foam stability. Figure 10E shows the impact of nanoparticle type on Neumann number in the absence of polymer at a constant concentration of salt and an anionic surfactant. As can be observed in this figure, in the absence of the polymer, different NPs show various effects on Ne. At the constant concentration of salt and surfactant, NPs are deposited from the interface due to insufficient stabilizers in the system. This causes irregularities in the charged clouds of contact surfaces and decreasing the osmotic repulsive forces[88], the long-range gravity forces increase and consequently stability decreases.

Comparison of the effectiveness of dimensionless numbers for evaluating foam stability

Through a comparative analysis of dimensionless numbers, it was observed that increase in the Ne, coupled with a decrease in the Bo and Wo, correlates with an improvement in foam stability. Concerning the Bo, the omission of consideration for the volume and height of the droplet, which affect surface tension, impedes a confident assertion regarding the specific nanoparticle contributing to foam stability. This discrepancy arises because research has revealed that the highest stability occurs for SiO_2, highlighting the limited accuracy of the Bo in showing the nanoparticles giving the most foam stability (Fig. 7A). Subsequently, it was proved that the most foam stability is related to Al_2O_3[42]. Within the Wo framework, accounting for the droplet volume in relation to surface has enhanced the precision of examining maximum foam stability. The findings show that the highest stability is linked to Al_2O_3 (Fig. 9A). The Ne stands out as the dimensionless number with the most precision in discerning foam stability. This numerical measure, excluding considerations for the impact of droplet height on surface tension, scrutinizes foam stability with greater accuracy compared to the Wo. The results conclusively point out Al_2O_3 being linked to the highest level of foam stability (Fig. 10A), supporting the previous conclusions[42].

While this study addressed various nanoparticle properties on foam stability, nanoparticle aggregation remains as a critical phenomenon in this context. Aggregation can either enhance and disrupt foam stability, depending on factors such as concentration, surface properties, and their interaction with surfactants. Proper aggregation can lead to the formation of stronger foams, whereas excessive aggregation may negatively affect stability. Therefore, further research is required to evaluate the impact of nanoparticle aggregation on foam stability, employing appropriate dimensionless numbers.

Conclusions

Experimental results demonstrate how dimensionless numbers can be used to characterize and predict foam stability across different systems and conditions. In the light of the investigations we have considered, these conclusions can be drawn:

The presence of nanoparticles (NPs) and other additives at optimal concentrations can enhance foam stability by reducing bubble growth rate and mass transfer between bubbles. Electrical conductivity serves as a reliable indicator of foam stability, with higher conductivity often signifying increased stability. The newly developed dimensionless conductivity number, De, effectively captures the impact of NPs surface charge on foam stability, with acidic NPs promoting better stability due to their enhanced absorption properties. Increasing Bo decreases lamella thickness, which can negatively impact foam stability by increasing gas mobility.

By considering droplet volume effect on IFT, foam stability measurements can be improved. NPs decrease gas diffusivity and increase lamella thickness, which enhances intermolecular forces and boost stability. The dimensionless number Ne, which consider droplet height and thin-film positioning, proves more effective than Bo and Wo for evaluating foam stability. Higher Ne values improve stability by altering force field positions and reducing gas bubble adhesion. Accurate drop-shape analysis leads to more precise IFT values and, consequently, more reliable foam stability measurements. Thus, Ne offers the highest accuracy, followed by Wo and Bo.

Data availability

The details of the calculations of dimensionless numbers are presented in the supplementary material.

Received: 21 September 2024; Accepted: 26 November 2024
Published online: 01 December 2024

References

1. Parsaei, R. & Chatzis, I. Experimental investigation of production characteristics of the gravity-assisted Inert Gas injection (GAIGI) process for Recovery of Waterflood Residual Oil: effects of Wettability Heterogeneity. *Energy Fuels*. **25** (5), 2089–2099 (2011).
2. Riazi, M., Sohrabi, M. & Jamiolahmady, M. Experimental study of pore-scale mechanisms of carbonated water injection. *Transp. Porous Media*. **86** (1), 73–86 (2011).
3. Lashkarbolooki, M., Riazi, M. & Ayatollahi, S. Experimental investigation of dynamic swelling and bond number of crude oil during carbonated water flooding; effect of temperature and pressure. *Fuel* **214**, 135–143 (2018).
4. Xiao, S. et al. Destabilization, Propagation, and generation of surfactant-stabilized foam during crude oil displacement in heterogeneous model porous media. Langmuir. ;34(3):739 – 49. (2018).
5. Bayat, A. E., Rajaei, K. & Junin, R. Assessing the effects of nanoparticle type and concentration on the stability of CO2 foams and the performance in enhanced oil recovery. *Colloids Surf., a*. **511**, 222–231 (2016).
6. Farzaneh, S. A. & Sohrabi, M. Experimental investigation of CO2-foam stability improvement by alkaline in the presence of crude oil. *Chem. Eng. Res. Des*. **94**, 375–389 (2015).
7. Kumar, S. & Mandal, A. Investigation on stabilization of CO2 foam by ionic and nonionic surfactants in presence of different additives for application in enhanced oil recovery. *Appl. Surf. Sci*. **420**, 9–20 (2017).

8. Guo, F. & Aryana, S. An experimental investigation of nanoparticle-stabilized CO2 foam used in enhanced oil recovery. *Fuel* **186**, 430–442 (2016).
9. Aronson, A. S., Bergeron, V., Fagan, M. E. & Radke, C. J. The influence of disjoining pressure on foam stability and flow in porous media. *Colloids Surf., a*. **83** (2), 109–120 (1994).
10. Choi, S. K., Son, H. A., Kim, H. T. & Kim, J. W. Nanofluid enhanced oil recovery using hydrophobically associative Zwitterionic polymer-coated silica nanoparticles. *Energy Fuels*. **31** (8), 7777–7782 (2017).
11. AlYousef, Z. A., Almobarky, M. A. & Schechter, D. S. The effect of nanoparticle aggregation on surfactant foam stability. *J. Colloid Interface Sci.* **511**, 365–373 (2018).
12. Olayiwola, S. O. & Dejam, M. A comprehensive review on interaction of nanoparticles with low salinity water and surfactant for enhanced oil recovery in sandstone and carbonate reservoirs. *Fuel* **241**, 1045–1057 (2019).
13. Rostami, P., Mehraban, M. F., Sharifi, M., Dejam, M. & Ayatollahi, S. Effect of water salinity on oil/brine interfacial behaviour during low salinity waterflooding: a mechanistic study. *Petroleum* **5** (4), 367–374 (2019).
14. Rezaeiakmal, F. & Parsaei, R. Visualization study of polymer enhanced foam (PEF) flooding for recovery of waterflood residual oil: Effect of cross flow. *J. Petrol. Sci. Eng.* **203**, 108583 (2021).
15. Rezaeiakmal, F., Parsaei, R., Shafiabadi, A. & Rezaei, A. Insights into the flow behaviour of the pre-generated polymer enhanced foam in heterogeneous porous media during tertiary oil recovery: Effect of gravitational forces. *J. Petrol. Sci. Eng.* **213**, 110385 (2022).
16. Shafiabadi, A., Parsaei, R., Rezaeiakmal, F. & Dehdari, B. Investigating the impact of wettability heterogeneity on tertiary oil recovery by foam flooding: a macroscopic visualization study. *Colloids Surf., a*. **675**, 132022 (2023).
17. Bernard, G. G. & Holm, L. W. Model study of Foam as a sealant for leaks in gas storage reservoirs. *Soc. Petrol. Eng. J.* **10** (01), 9–16 (1970).
18. Hirasaki, G. J. et al. Field demonstration of the surfactant/foam process for aquifer remediation. *SPE Annual Technical Conference and Exhibition*. :SPE-39292-MS. (1997).
19. Li, S. Y., Li, Z. M. & Li, B. F. Experimental study of the effect of permeability on foam diversion. *Pet. Sci. Technol.* **30** (18), 1907–1919 (2012).
20. Cheng, L., Kam, S. I., Delshad, M. & Rossen, W. R. Simulation of dynamic foam-acid diversion processes. *SPE J.* **7** (03), 316–324 (2002).
21. Amirian, E., Dejam, M. & Chen, Z. Performance forecasting for polymer flooding in heavy oil reservoirs. *Fuel* **216**, 83–100 (2018).
22. Saboorian-Jooybari, H., Dejam, M. & Chen, Z. Heavy oil polymer flooding from laboratory core floods to pilot tests and field applications: half-century studies. *J. Petrol. Sci. Eng.* **142**, 85–100 (2016).
23. Hurtado, Y. et al. Effects of Surface Acidity and polarity of SiO2 nanoparticles on the Foam Stabilization Applied to Natural Gas flooding in tight gas-condensate reservoirs. *Energy Fuels*. **32** (5), 5824–5833 (2018).
24. Rahman, A., Torabi, F. & Shirif, E. Surfactant and nanoparticle synergy: towards improved foam stability. *Petroleum* (2023).
25. Zhang, T. et al. Engineered nanoparticles as harsh-condition emulsion and foam stabilizers and as novel sensors. *Offshore Technology Conference*. 2011:OTC-21212-MS.
26. Rafati, R., Hamidi, H., Idris, A. K. & Manan, M. A. Application of sustainable foaming agents to control the mobility of carbon dioxide in enhanced oil recovery. *Egypt. J. Petroleum*. **21** (2), 155–163 (2012).
27. Sun, Q. et al. Aqueous foam stabilized by partially hydrophobic nanoparticles in the presence of surfactant. *Colloids Surf., a*. **471**, 54–64 (2015).
28. Medina, O. E. et al. Improvement of steam injection processes through nanotechnology: an approach through in situ upgrading and foam injection. *Energies* 12. (2019).
29. Suleymani, M., Ghotbi, C., Ashoori, S., Moghadasi, J. & Kharrat, R. Theoretical and experimental study of foam stability mechanism by nanoparticles: Interfacial, bulk, and porous media behavior. *J. Mol. Liq.* **304**, 112739 (2020).
30. Farajzadeh, R., Andrianov, A., Krastev, R., Hirasaki, G. J. & Rossen, W. R. Foam–oil interaction in porous media: implications for foam assisted enhanced oil recovery. *Adv. Colloid Interface Sci.* **183–184**, 1–13 (2012).
31. Yan, W., Miller, C. A. & Hirasaki, G. J. Foam sweep in fractures for enhanced oil recovery. *Colloids Surf., a* ;282–283 :348–59. (2006).
32. Amani, P., Miller, R., Javadi, A. & Firouzi, M. Pickering foams and parameters influencing their characteristics. *Adv. Colloid Interface Sci.* **301**, 102606 (2022).
33. Kumar, D., Lashari, N., Ganat, T., Ayoub, M. A., Soomro, A. A., & Chandio, T. A. (2022).A review on application of nanoparticles in cEOR: Performance, mechanisms, and influencing parameters. *Journal of Molecular Liquids*, *353*, 118821.
34. Lashari, N. & Ganat, T. Emerging applications of nanomaterials in chemical enhanced oil recovery: Progress and perspective. *Chin. J. Chem. Eng.* **28** (8), 1995–2009 (2020).
35. Lashari, N., Ganat, T., Elraies, K. A., Ayoub, M. A., Kalam, S., Chandio, T. A., …Sharma, T. (2022). Impact of nanoparticles stability on rheology, interfacial tension,and wettability in chemical enhanced oil recovery: A critical parametric review. *J. Petroleum Sci. Eng.*, *212*, 110199.
36. Kumar, D., Ganat, T., Lashari, N., Ayoub, M. A., Kalam, S., Chandio, T. A., & Negash,B. M. (2022). Experimental investigation of GO-HPAM and SiO2-HPAM composite for cEOR:Rheology, interfacial tension reduction, and wettability alteration. *Colloids and Surfaces A: Physicochemical and Engineering Aspects*, *637*, 128189.
37. Farhadi, H., Riahi, S., Ayatollahi, S. & Ahmadi, H. Experimental study of nanoparticle-surfactant-stabilized CO2 foam: Stability and mobility control. *Chem. Eng. Res. Des.* **111**, 449–460 (2016).
38. Panahpoori, D., Rezvani, H., Parsaei, R. & Riazi, M. A pore-scale study on improving CTAB foam stability in heavy crude oil – water system using TiO2 nanoparticles. *J. Petrol. Sci. Eng.* **183**, 106411 (2019).
39. Rezvani, H. et al. A novel foam formulation by Al2O3/SiO2 nanoparticles for EOR applications: a mechanistic study. *J. Mol. Liq.* **304**, 112730 (2020).
40. Derikvand, Z. & Riazi, M. Experimental investigation of a novel foam formulation to improve foam quality. *J. Mol. Liq.* **224**, 1311–1318 (2016).
41. Harati, S., Esfandyari Bayat, A. & Sarvestani, M. T. Assessing the effects of different gas types on stability of SiO2 nanoparticle foam for enhanced oil recovery purpose. *J. Mol. Liq.* **313**, 113521 (2020).
42. Dehdari, B., Parsaei, R., Riazi, M., Rezaei, N. & Zendehboudi, S. New insight into foam stability enhancement mechanism, using polyvinyl alcohol (PVA) and nanoparticles. *J. Mol. Liq.* **307**, 112755 (2020).
43. Sun, L. et al. Recent advances of surfactant-stabilized N2/CO2 foams in enhanced oil recovery. *Fuel* **241**, 83–93 (2019).
44. Hurtado, Y., Franco, C. A., Riazi, M. & Cortés, F. B. Improving the stability of nitrogen foams using silica nanoparticles coated with polyethylene glycol. *J. Mol. Liq.* **300**, 112256 (2020).
45. Yan, T., Song, B., Cui, Z. & Pei, X. Highly wet aqueous foams stabilized by an amphiphilic bio-based hydrogelator derived from dehydroabietic acid. *Soft Matter*. **16** (9), 2285–2290 (2020).
46. Du, D. et al. Parameter screening study for optimizing the Static properties of nanoparticle-stabilized CO2 foam based on Orthogonal Experimental Design. *ACS Omega*. **5** (8), 4014–4023 (2020).
47. Kamal, M. S. A Novel approach to stabilize foam using fluorinated surfactants. *Energies* 12. (2019).
48. Beheshti, E., Riahi, S. & Riazi, M. Impacts of oil components on the stability of aqueous bulk CO2 foams: an experimental study. *Colloids Surf., a*. **648**, 129328 (2022).

49. Saeedi Dehaghani, A. H., Gharibshahi, R. & Mohammadi, M. Utilization of synthesized silane-based silica Janus nanoparticles to improve foam stability applicable in oil production: static study. *Sci. Rep.* **13** (1), 18652 (2023).
50. Chen, H. et al. Oil effect on CO2 foam stabilized by a switchable amine surfactant at high temperature and high salinity. *Fuel* **227**, 247–255 (2018).
51. Amirmoshiri, M. et al. Probing the effect of oil type and saturation on foam flow in porous media: core-flooding and nuclear magnetic resonance (NMR) imaging. *Energy Fuels*. **32** (11), 11177–11189 (2018).
52. Jian, G. et al. Evaluating the transport behavior of CO2 foam in the presence of crude oil under high-temperature and high-salinity conditions for carbonate reservoirs. *Energy Fuels*. **33** (7), 6038–6047 (2019).
53. Du, D. et al. Experimental study on rheological properties of nanoparticle-stabilized carbon dioxide foam. *J. Nat. Gas Sci. Eng.* **75**, 103140 (2020).
54. Zhang, P. et al. Experimental investigation of amine-surfactant CO2 foam for smart mobility control during CO2 flooding. *J. Petrol. Sci. Eng.* **184**, 106511 (2020).
55. Li, Q. & Prigiobbe, V. Studying the generation of foam in the presence of nanoparticles using a microfluidic system. *Chem. Eng. Sci.* **215**, 115427 (2020).
56. Lv, Q. et al. Enhanced oil recovery using aqueous CO2 Foam stabilized by particulate matter from coal combustion. *Energy Fuels* **34** (3), 2880–2892 (2020).
57. Conn, C. A., Ma, K., Hirasaki, G. J. & Biswal, S. L. Visualizing oil displacement with foam in a microfluidic device with permeability contrast. *Lab. Chip*. **14** (20), 3968–3977 (2014).
58. Rahman, A., Shirif, E. & Torabi, F. Nanoparticle-stabilized CO2 foam flooding for enhanced heavy oil recovery: A micro-optical analysis. *Petroleum*. (2024).
59. Morton, B. R., Units, Dimensions & Numbers, D. By D. C. IPSEN. New York: McGraw-Hill Book Co., 236 pp. 50s. 6d. Journal of Fluid Mechanics 1960;9(4):478 – 80. (1960).
60. Ruzicka, M. C. On dimensionless numbers. *Chem. Eng. Res. Des.* **86** (8), 835–868 (2008).
61. Eggers, J. & Villermaux, E. Physics of liquid jets. *Rep. Prog. Phys.* **71** (3), 036601 (2008).
62. Bois, R. et al. Influence of process variables on foaming ability of surfactants: experimental study and dimensional analysis. *Chem. Eng. Res. Des.* **165**, 40–50 (2021).
63. Tiwari, S. et al. *Foaming Prediction in Pure Liquids from Dimensionless Numbers Inspired* (by the Theory of Fluid Behavior for Drops, 2023).
64. WorthingtonAM & StewartB (ed) On pendent drops. *Proc. Royal Soc. Lond.* **32** 212-215 362–377 (1881).
65. Yang, J., Yu, K. & Zuo, Y. Y. Accuracy of axisymmetric drop shape analysis in determining surface and interfacial tensions. *Langmuir* **33** (36), 8914–8923 (2017).
66. Rotenberg, Y., Boruvka, L. & Neumann, A. W. Determination of surface tension and contact angle from the shapes of axisymmetric fluid interfaces. *J. Colloid Interface Sci.* **93** (1), 169–183 (1983).
67. Río OId, Neumann, A. W. Axisymmetric Drop shape analysis: computational methods for the measurement of Interfacial properties from the shape and dimensions of pendant and Sessile drops. *J. Colloid Interface Sci.* **196** (2), 136–147 (1997).
68. Bashforth, F. & Adams, J. C. *An Attempt to test the Theories of Capillary Action* (University, 1883).
69. Merrington, A. C. & Richardson, E. G. The break-up of liquid jets. Proceedings of the physical society. ;59(1):1. (1947).
70. Li, S., Liu, M., Hanaor, D. & Gan, Y. Dynamics of viscous entrapped saturated zones in partially wetted porous media. *Transp. Porous Media*. **125** (2), 193–210 (2018).
71. Berry, J. D., Neeson, M. J., Dagastine, R. R., Chan, D. Y. C. & Tabor, R. F. Measurement of surface and interfacial tension using pendant drop tensiometry. *J. Colloid Interface Sci.* **454**, 226–237 (2015).
72. Ghosh, P. *Colloid and Interface Science* (PHI Learning Pvt. Ltd., 2009).
73. Jones, S. A., van der Bent, V., Farajzadeh, R., Rossen, W. R. & Vincent-Bonnieu, S. Surfactant screening for foam EOR: correlation between bulk and core-flood experiments. *Colloids Surf., a*. **500**, 166–176 (2016).
74. Kabalnov, A. Ostwald ripening and related phenomena. *J. Dispers. Sci. Technol.* **22** (1), 1–12 (2001).
75. Georgieva, D., Cagna, A. & Langevin, D. Link between surface elasticity and foam stability. *Soft Matter*. **5** (10), 2063–2071 (2009).
76. Fowkes, F. M. Additivity of intermolecular forces at interfaces. i. determination of the contribution to surface and interfacial tensions of dispersion forces in various liquids1. *J. Phys. Chem.* **67** (12), 2538–2541 (1963).
77. Guldbrand, L., Jönsson, B., Wennerström, H. & Linse, P. Electrical double layer forces. A Monte Carlo study. *J. Chem. Phys.* **80** (5), 2221–2228 (1984).
78. Hove, A. O., Dawe, R. A. & Evans, R. N. Gravity segregation at the pore scale in cores under miscible and low interfacial tension conditions including in-situ tomography. *J. Petrol. Sci. Eng.* **14** (1–2), 89–98 (1995).
79. Li, S., Liu, M., Hanaor, D. & Gan, Y. Dynamics of viscous entrapped saturated zones in partially wetted porous media. *Transp. Porous Media*. **125**, 193–210 (2018).
80. Okesanjo, O., Meredith, J. C. & Behrens, S. H. Effect of shear on pumped capillary foams. *Ind. Eng. Chem. Res.* **62** (18), 7031–7039 (2023).
81. Prieve, D. C. & Ruckenstein, E. Effect of London forces upon the rate of deposition of Brownian particles. *AIChE J.* **20** (6), 1178–1187 (1974).
82. Nickdel Teymoori, R. & Ghasem Alaskari, M. K. Effects of salinity, pH and temperature on CMC Polymer and XC Polymer performance. *Int. J. Eng.* **20** (3), 283–290 (2007).
83. Hu, N. et al. Foams stabilization by silica nanoparticle with cationic and anionic surfactants in column flotation: effects of particle size. *J. Taiwan Inst. Chem. Eng.* **88**, 62–69 (2018).
84. Quoc, P. N., Zitha, P. L. & Currie, P. K. Effect of foam films on gas diffusion. *J. Colloid Interface Sci.* **248** (2), 467–476 (2002).
85. Kazemzadeh, Y., Dehdari, B., Etemadan, Z., Riazi, M. & Sharifi, M. Experimental investigation into Fe3O4/SiO2 nanoparticle performance and comparison with other nanofluids in enhanced oil recovery. *Pet. Sci.* **16** (3), 578–590 (2019).
86. Rezvani, H., Kazemzadeh, Y., Sharifi, M., Riazi, M. & Shojaei, S. A new insight into Fe3O4-based nanocomposites for adsorption of asphaltene at the oil/water interface: an experimental interfacial study. *J. Petrol. Sci. Eng.* **177**, 786–797 (2019).
87. Giorgi, F., Coglitore, D., Curran, J. M., Gilliland, D., Macko, P., Whelan, M., …Patterson, E. A. (2019). The influence of inter-particle forces on diffusion at the nanoscale. *Sci. Rep. 9*(1), 12689.
88. Langevin, D. Recent advances on emulsion and foam stability. *Langmuir* **39** (11), 3821–3828 (2023).

Acknowledgements

The cooperation of the EOR research center of Shiraz University in this study is acknowledged.

Author contributions

Conceptualization: R.P. and M.R.Methodology: B.D., R.P., and M.R.Software: BDValidation: BDFormal analysis: BDInvestigation: BD, Resources: RP, MRData Curation: BD, RPWriting - Original Draft: BDWriting - Review & Editing: RP, MR, MNVisualization: BDSupervision: RP, MRProject administration: RP, MRFunding acquisition: RP, MR.

Declarations

Competing interests
The authors declare no competing interests.

Additional information
Correspondence and requests for materials should be addressed to R.P.

Reprints and permissions information is available at www.nature.com/reprints.

Publisher's note Springer Nature remains neutral with regard to jurisdictional claims in published maps and institutional affiliations.